Supplement of Hydrol. Earth Syst. Sci., 29, 6647–6662, 2025 https://doi.org/10.5194/hess-29-6647-2025-supplement © Author(s) 2025. CC BY 4.0 License.





# Supplement of

# Robust adaptive pathways for long-term flood control in delta cities: addressing pluvial flood risks under future deep uncertainty

Hengzhi Hu et al.

Correspondence to: Jiahong Wen (jhwen@shnu.edu.cn)

The copyright of individual parts of the supplement might differ from the article licence.

## **Contents of this file**

- S1 Data and scenarios
- S2 Inundation risk and solution performance
- S3 Risk assessment
- **S4** Benefit-cost analysis
- Figure S1 Structure of SUIM model
- Figure S2 Comparison of damage/loss
- Table S1 Data information description
- Table S2 Future uncertain factors and range of uncertainties in 2050
- **Table S3** Simulation setting-up to the performance of adaptation measures
- **Table S4** Statistic information of measures combinations
- Table S5 Depth-damage curve of inundation depth in Shanghai
- Table S6 Life cycle cost estimates for five adaptation measures
- Table S7 Metrics' value of all measures for multi-objective analysis

#### S1 Data and scenarios

First, we built a database based on multi-source data such as basic geographic information, meteorological and hydrological data, and urban hydrological flood control data. The data in this study include rainfall data, drainage capacity data, elevation data, socioeconomic statistics, land use data (Table S1).

- 1) Rainfall data. The hourly rainfall data of 11 meteorological stations in Shanghai, including Xujiahui (representing the central urban area), Minhang, Baoshan, Pudong, Jiading, Nanhui (now part of Pudong New Area), Jinshan, Qingpu, Songjiang, Fengxian and Chongming, were taken from 16:00 to 19:00 on September 13, 2013. The station observation data are spatially interpolated to the 30m resolution grid as the precipitation input data of the model. The diachronic precipitation data of 11 stations in the central urban area and counties of Shanghai center were collected to study the temporal variation trend and spatial distribution characteristics of each diachronic extreme precipitation. In addition, this study also collected the "110" citizen alarm records during the "913" period as the model simulation verification data, which includes the location of alarm points and the submergence depth of alarm points.
- 2) Drainage Capacity Data. In terms of municipal drainage, due to the lack of pipeline data, this study uses the generalized 2013 Shanghai drainage capacity data to characterize the design standards of each drainage unit. The central urban area in the outer ring road of Shanghai is divided into 284 drainage units, and its drainage capacity is divided into three categories. Among them, those with poor drainage capacity are generally the old designed rainwater sewage combined pipe network in the main urban area, and the design standard is 27mm/h. Other new drainage units are basically designed according to the one-year rainstorm standard, and the drainage capacity is 36mm/h; In addition, the designed drainage capacity of the Expo site is 50mm/h.
- **3)** Elevation data. The digital elevation model (DEM) data in this study has a resolution of 30m, which is based on detailed observation results of NASA's new generation earth observation satellite Terra. On the basis of the source data, the filling of depressions is used to remove some false depressions. The data of residential and commercial types are extracted according to the land use data, and the elevation of 15mm is corrected.

- 4) Socioeconomic Statistics. It mainly comes from the "Shanghai Statistical Yearbook" published by the Shanghai Municipal Bureau of Statistics every year. The entries include district and county population, district and county GDP, public green area, average household properties and average construction cost.
- 5) Land use data. The land use data adopts the remote sensing monitoring data of China's land use status in 2015 released by the Institute of Geographical Sciences and Resources, Chinese Academy of Sciences. The 30m resolution land use data of Shanghai in the study were selected. It includes 9 categories and 32 types of land use. The study redivided the above categories into 10 types of land use, including industrial and commercial land, new-style residences, and natural villages.

Table S1 Data information description

Type of data	Data resolution	Data description
Rainfall information	30m	Hourly rainfall data from 11 weather stations
Drainage capacity	Shapefile	284 drainage units with design standards of
		27mm/h, 36mm/h and 50mm/h respectively.
Elevation	30m	Advanced Spaceborne Thermal Emission and
		Anti-Radiometer GDEM Data with ASTER
		Sensors
Socioeconomic	Shapefile	District and sub-district population, district and
Statistics		county GDP, area and investment of public
		green space, average indoor property and
		average construction cost
land use	30m	Industrial land, commercial land, new housing

#### **Scenarios generation**

Three uncertainty factors, future rainfall ( $\alpha$ ), the urban rain island effect ( $\beta$ ), and the decrease of drainage capacity ( $\gamma$ ), have been selected to generate future extreme rainstorm scenarios (Table S2). The range (between 7% and 18%) of the future rainfall ( $\alpha$ ) is derived from daily down-scaled dataset of 21 GCM simulations of CMIP5 (under both RCP4.5 and RCP8.5 emission scenarios) in Yangtze River Delta region, with nine grid-cells covering Shanghai city by 2050(Wu et al., 2018). For the urban rain island effect ( $\beta$ ), the previous work (Liang and Ding, 2017) found that total precipitation amounts of heavy rainfall event over central urban (Pudong and Xujiahui) and nearby suburban (Minhang and Jiading) sites increased by the rates of 21.7-25mm/10yr, which have a proximate margin of increase ( $\beta$ 1) by 10% to 20% in the case of future reoccurrence over central urban sites (Xujiahui and Pudong) by the 2050s, but will have a small margin of decrease ( $\beta$ 2) by -0.076% to -0.038%

at other stations. To take into account the uncertainties in sea-level rise, land subsidence, and other degradation factors of the drainage systems, we assume that the decreasing rate of existing drainage system capability (g) would range between 0% and 50% (Hu et al., 2019). Based on the ranges of three uncertain factors, there are 100 scenarios are generated via Latin Hyper Cube Sampling (LHS), more details can be found in Hu et al. (2019).

**Table S2.** Future uncertain factors and range of uncertainties in 2050

Uncertain factors	Range of uncertainties
Future rainfall (α)	(α)increase from 7% to 18%
Urban rain island effect $(\beta)$	( $\beta$ )increase from 10% to 20% in central region (Xujiahui and Pudong rain gauges), decrease from -0.076% to -0.038% (other 9 rain gauges in Shanghai)
Decrease of drainage capacity (γ)	(γ) decrease from 0 to 50% due to the anthropogenic land subsidence and sea level rise

#### S2 Inundation risk and option's performance

The hydrological model of SCS-CN (Soil Conservation Service Curve Number) has the characteristics of simple parameters and easy access to data, which has been widely applied in Shanghai. Hu et al., (2023) established the Shanghai Urban Inundation Model (SUIM) based on SCS-CN in order to address the challenges of multi-scenario, multi-model, and large-scale simulation calculations. It aims to establish a rapid and integrated model for minimizing risk, and to offer technical support for assessing the capacities of adaptation measures in mitigating urban pluvial flood risk.

The SUIM encapsulates the sub-modules of rainfall module, hydrology module, spatial statistics module, risk assessment module, and measure evaluation module to provide technical solutions for integrated risk assessment and measure evaluation. The coupled sub-modules can optimize the simulation process and computing efficiency. The model adopts a PostgreSQL database that supports GIS spatial data storage. It supports GIS spatial analysis and calculation, including clipping of features, extraction of layers, coordinate transformation, and spatial interpolation. The model's underlying data employ a regular grid structure, which has the advantages of speedy calculation, simple logic operation, and automatic processing capability. The integrated model is suitable for various applications, including backtracking of historical events, early warning of inundation

forecasting, future scenario evaluation, and pre-planning of hydraulic engineering. The overall structure of SUIM model is shown in Figure S1.

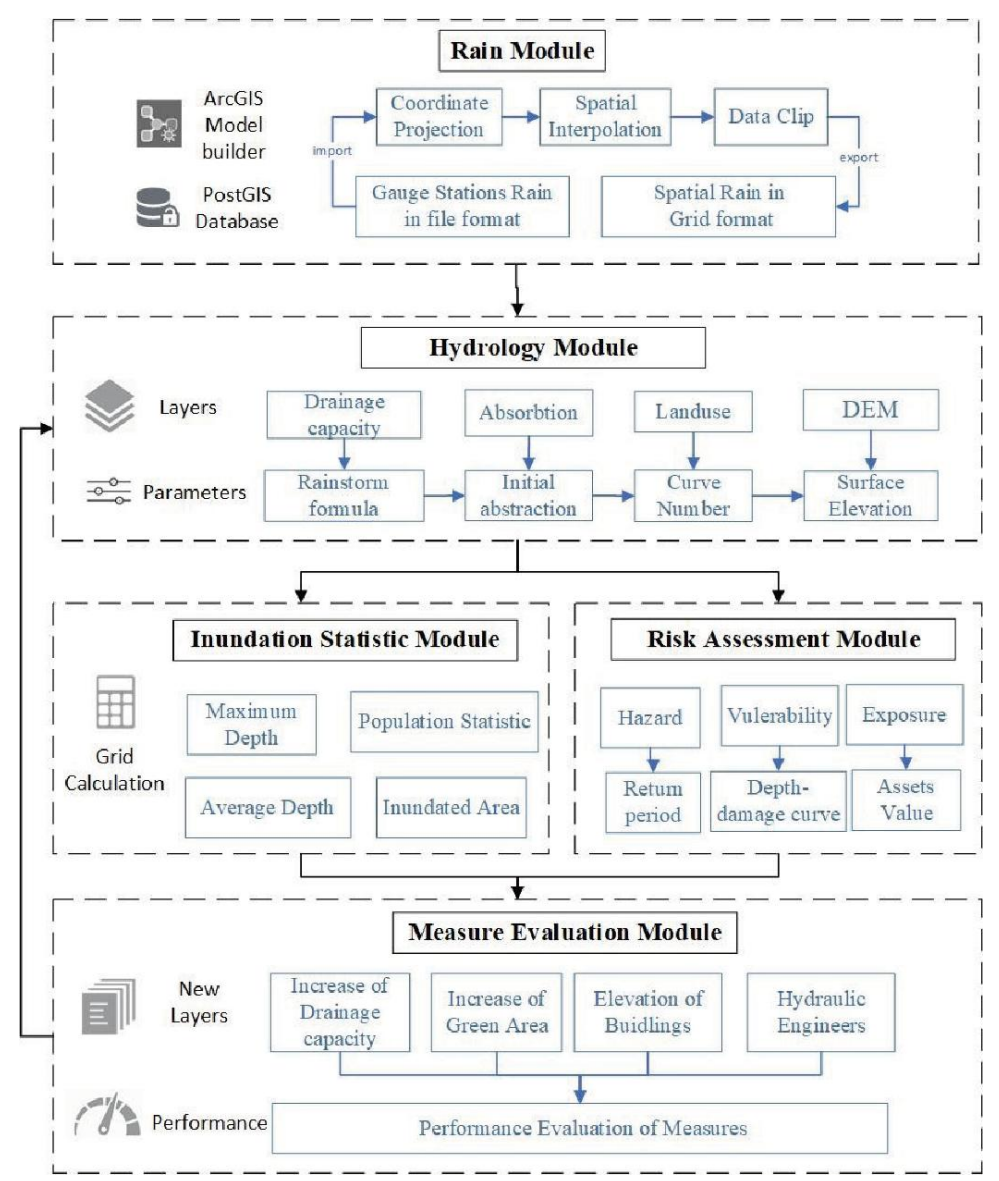
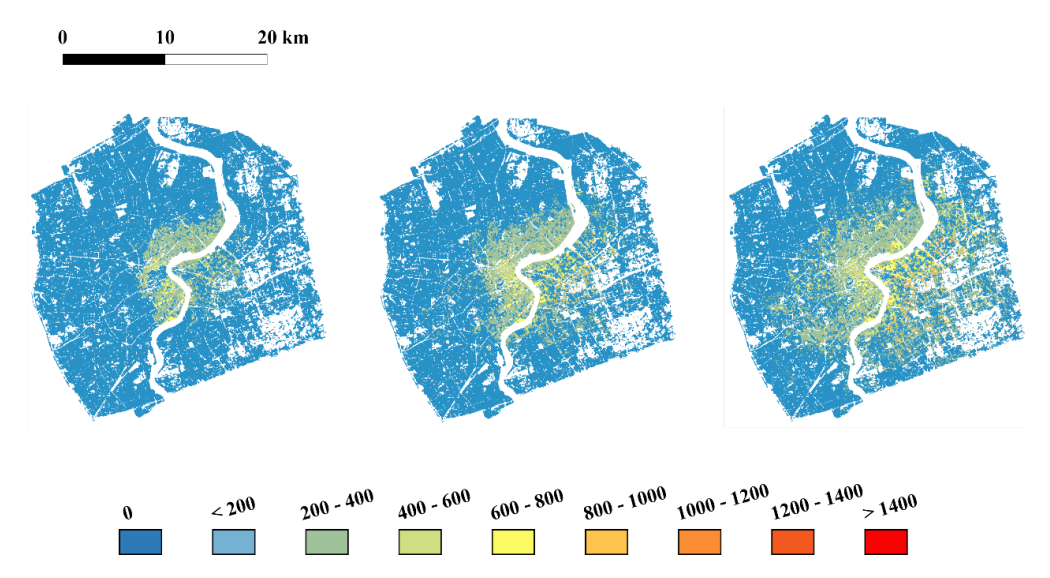


Figure S1 Structure of SUIM model(Hu et al., 2023)

Hu et al. (2019) evaluated the inundation loss under 100 plausible futures (Figure S2). To compare and quantitatively evaluate the performance of adaptation options, they simulated the differences in maximum waterlogging depth resulting from the implementation of these adaptation measures. In addition to the baseline scenario, 100 futures were simulated for each adaptation option and its combinations. The specific simulation parameters and performance results are presented in Tables S3 and S4.



**Figure S2**. Comparison of damage/loss (thousand RMB/900m<sup>2</sup> grid): Sc-53 (left), Sc-3 (middle), Sc-11 (right)(Hu et al., 2019)

**Table S3** Simulation setting-up to the performance of adaptation measures

Experiment	Option	Experimental program	Performance	Abbreviation
0	baseline	Model effect verification	/	_
1	baseline	City Defense Capability Simulation	/	
2	Drainage	Increase drainage capacity to 1/5-year	low	Dr
3	Green area	Increase surface water permeability	low	GA
4	deep tunnel 1	absorb 30% of rainfall	middle	Tun30
5	deep tunnel 2	absorb 50% of rainfall	middle	Tun50
6	deep tunnel 3	absorb 70% of rainfall	high	Tun70
7	Combination 1	Green area + Drainage	middle	D+G
8	Combination 2	Green area + Deep tunnel 1	middle	G+Tun30
9	Combination 3	Green area + Deep tunnel 2	high	G+Tun50
10	Combination 4	Green area + Deep tunnel 3	overflow	G+Tun70
11	Combination 5	Drainage + Deep tunnel 1	middle	D+Tun30
12	Combination 6	Drainage + Deep tunnel 2	high	D+Tun50
13	Combination 7	Drainage + Deep tunnel 3	overflow	D+Tun70
14	Combination 8	Green area + Drainage + Deep tunnel 1	high	D+G+Tun30
15	Combination 9	Green area + Drainage + Deep tunnel 2	overflow	D+G+Tun50
16	Combination 10	Green area + Drainage + Deep tunnel 3	overflow	D+G+Tun70

Table S4 Statistic information of measures combinations

Min	25%	Mid	75%	Max	Std	Mean	Range

Dr	0.08	0.11	0.16	0.37	0.80	0.20	0.25	0.72
GA	0.09	0.11	0.17	0.38	0.73	0.18	0.26	0.64
Tun30	0.17	0.20	0.32	0.54	0.89	0.21	0.39	0.72
D+G	0.18	0.37	0.70	0.89	0.94	0.27	0.62	0.76
Tun50	0.33	0.65	0.85	0.91	0.99	0.21	0.74	0.66
D+G+T30	0.61	0.80	0.89	0.91	0.99	0.08	0.85	0.38
Tun70	0.79	0.81	0.89	0.91	0.99	0.05	0.87	0.2

#### S3 Risk assessment

The assessment of asset value includes commercial asset value, i.e., commercial and residential buildings, and household property. Exposure analysis is performed by overlaying flood scenarios and asset values across multiple scenarios. The calculation formula is:

$$B_{\text{exp} \, \text{osure}} = A_{\text{asset}} \cap H \tag{S1}$$

where  $B_{exposure}$  is the exposed assets;  $A_{asset}$  is the value of land use assets; and H is hazard.

A comprehensive evaluation of exposure of assets including indoor property, business and building losses with depth-damage curve. Based on the results of previous studies (Ke, 2014), this study established an inundation depth-vulnerability curve suitable for the study area, as shown in Table S5.

Table S5 Depth-damage curve of inundation depth in Shanghai

Category	Inundation depth (m)							
	< 0.5	0.5-1.0	1.0-1.5	1.5-2.0	2.0-2.5	2.5-3.0	>3.0	
Public building	3%	7%	12%	14%	18%	20%	25%	
Commercial	5%	9%	13%	18%	22%	27%	31%	
Building								
Industrial	3%	8%	11%	15%	19%	2%	25%	
building								
Residential	3%	65	9%	12%	16%	19%	22%	
building								
Household	9%	19%	26%	33%	38%	46%	58%	
property								

The damage loss of pluvial flood is calculated in SUIM by each inundation of the scenarios. The statistic information is then calculated at grid level.

$$T_{loss} = \sum_{i=1, j=1}^{n} (V_i \times R_j)$$
 (S2)

where  $T_{loss}$  is the total loss in the study region;  $V_i$  is the *i-th* exposed asset value of the elements at risk;  $R_j$  is the *j-th* loss rate of the elements at risk in different water depth intervals.

To evaluate the flood control options, the inundation statistic is quantified by resimulation in the baseline scenario in SUIM. For example, the performance of measures of drainage capacity enhancement can be calculated as the loss reduction rate compared to baseline measures under future scenarios.

$$RRR = \frac{T_{loss}' - T_{loss}}{T_{loss}} \times 100\%$$
 (S3)

where  $T_{loss}$ ' is the flood damage after implementing a flood control measure; accordingly, *Performance* calculates the reduction rate of loss against its baseline scenario.

### S4 Benefit-cost analysis

Benefit and cost are indispensable considerations when making investments. Typically, the cost of a measure is proportional to its benefit (flood risk reduction). Engineered solutions with superior performance typically incur higher cost and longer construction period. This study evaluates the economic viability of various options by calculating their cost-benefit ratios. In terms of cost assessment, the life cycle cost analysis method (LCCA) is introduced, which takes into account the initial construction cost of various measures, the average annual use and maintenance cost, the residual value of the facility when the end of its service period approaches, and the effective period of the facility. In Table S6 of the Supplementary Material, the cost of the measure is determined using LCCA. Internationally, the net present value of benefits (PVB) and the net present value of costs (PVC) are utilized to represent benefits and expenses, respectively (Xie et al., 2017). The formula for calculating benefit-cost ratio is as follows:

$$\frac{B}{C} = \frac{PVB}{PVC} \tag{S4}$$

Considering that the goal of this study is not to calculate the direct risk of extreme waterlogging in the future, and the absolute value of the risk is too large to be comparable, the net present value of the benefit PVB is selected as the inundation risk reduction rate (RRR) before and after the implementation of the measures, rather than the waterlogging risk reduction value. The life cycle cost analysis formula is as follows:

$$PVC_{Y} = IC_{Y} + \sum_{t=0}^{T} fr_{t}MO_{t} - fr_{T}SV_{t}$$
 (S5)

The costing of measures includes initial cost (IC), annual maintenance and operations (MO) and residual value (SV);  $fr_t$  is the present value factor for the discount rate r in a particular year t; the present value factor for the discount rate r at the end of r years in the design life of  $fr_T$ . The life cycle is designed to be 20-50 years, and the investment horizon is T years. Taking into account the economic growth rate, the study assumes a discount rate of 5% in Shanghai (Ke, 2015). For simplicity, costs of options were not discounted in our analysis, and we treated all monetary values in constant terms

We used life cycle cost analysis to evaluate the cost of five adaptation options, includes the drainage enhancement (Dr), public green area (GA), the 30% absorption capacity of the deep tunnel (Tun30), the 50% absorption capacity of the deep tunnel (Tun50), and the 70% absorption capacity of the deep tunnel (Tun70). Table S6 presents that the LCCA the order from low to high: Dr < Tun30 < GA < Tun50 < Tun70. Dr has the lowest total cost, while Tun70 (70% deep tunnel capacity) has the highest cost.

From the perspective of annual average cost (AAC), the order of cost from low to high is: GA <Dr < Tun30 <Tun50<Tun70. The AAAC of low impact solutions for "public green area" is the lowest, and the average annual cost of "grey" option is high. In addition to these five basic options, two combined options were analyzed: (Dr + GA) "drainage enhancement + public green area increase" and (Dr + GA + Tun30) "drainage enhancement + public green area increase + 30% absorption capacity of deep tunnels." Their AAC and total costs were also calculated.

The results in Table S6 show that the individual measures of drainage enhancement (Dr), public green area (GA), and the 30% deep tunnel (Tun30) have similar Average Annual Costs (AAC) (37-41 million USD/year) and total costs in a comparable range (1918-2570 million USD). However, their average risk reduction rates (ARRR) are low (less than 0.39, Table 2), indicating unsatisfactory performance in extreme flooding scenarios. In terms of risk reduction, the combined measure (Dr + GA) shows a higher rate (0.62, Table 2) than the single measures, indicating that the benefits of combined options are greater. Although the Tun50 and Tun70 options have relatively high AAC and total costs—lower only than the combined (Dr + GA) and (Dr + GA + Tun30) measures—their

average risk reduction rates (ARRR) are also relatively high(above 0.74).

Table S6 Life cycle cost estimates for five adaptation options

Measure	Unit cost (million/km, million/km <sup>2</sup> )	Unit (km,km <sup>2</sup>	Mainten ance costs	Life span	Total cost (million)	Residual value (million)	Average annual cost (million)
Dr	14	118	2%	50	1,918	52	39
GA	86	30	2%	70	2,570	36	37
Tun30	43	22	5%	50	2,010	29	41
Tun50	43	37	5%	50	3,350	49	68
Tun70	43	52	5%	50	4,690	68	95

<sup>\*</sup>Note: Considering that public green space generally does not have a useful life period, the period is set to 70 years. The cost of Dr and GA is referred to Xie et al., 2017

For the multi-objective analysis (Table S7), all metric values for the single options and their combinations were normalized from 0 to 1 and then equally weighted to create a sum score. The results show that Tun50 achieves the best benefit-cost ratio (BCR), while Tun70 has the highest ARRR and valid period. In comparison, the combined measure (Dr + GA + Tun30) has the highest flexibility and the highest final sum score, indicating the best overall performance among all options.

Table S7 Metrics' value of all measures for multi-objective analysis

Measure	GA	Dr	Tun30	D+G	Tun50	D+G+Tun30	Tun70
ARRR	0	0.10	0.47	0.50	1.00	0.90	0.93
BCR	0.12	0.00	0.70	0.38	1.00	0.19	0.61
Flexibility	0	0	0	0.67	0.33	1.00	0.33
Valid period	0.08	0.14	0.20	0.22	0.58	0.96	1.00
Sum score	0.22	0.26	1.38	1.77	2.91	3.05	2.87

#### Reference

- Hu, H., Yang, H., Wen, J., Zhang, M., and Wu, Y.: An Integrated Model of Pluvial Flood Risk and Adaptation Measure Evaluation in Shanghai City, Water, 15(3), 602, https://doi.org/10.3390/w15030602, 2023.
- Hu, H. Z., Tian, Z., Sun, L. X., Wen, J., Liang, Z., Dong, G., and Liu, J.: Synthesized trade-off analysis of flood control solutions under future deep uncertainty: An application to the central business district of Shanghai, Water Research, 166, 115067, https://doi.org/10.1016/j.watres.2019.115067, 2019.
- Ke, Q.: Flood Risk Analysis for Metropolitan Areas A Case Study for Shanghai, PhD Dissertation, Technology of Delft University, Department of Hydraulic Engineering, 2014.
- Liang, P., and Ding, Y. H.: The long-term variation of extreme heavy precipitation and its link to urbanization effects in Shanghai during 1916-2014, Adv. Atmos. Sci., 34, 321-334, https://doi.org/10.1007/s00376-016-6120-0, 2017.
- Wu, W., Liang, Z., and Liu, X.: Projection of the daily precipitation using CDF-T method at meteorological observation site scale, Plateau Meteorology, 37(3), 796-805, 2018. (In Chinese).
- Xie, J., Chen, H., Liao, Z., Gu, X., Zhu, D., and Zhang, J.: An integrated assessment of urban flooding mitigation strategies for robust decision making, Environmental Modelling & Software, 95, 143-155, https://doi.org/10.1016/j.envsoft.2017.06.027, 2017.